Infrared-to-visible and infrared-to-violet upconversion fluorescence of rare earth doped LaF_3 nanocrystals

2008 Chinese Phys. B 17 3300

(http://iopscience.iop.org/1674-1056/17/9/026)

Vol 17 No 9, September 2008
1674-1056/2008/17(09)/3300-06

Chinese Physics B

Infrared-to-visible and infrared-to-violet upconversion fluorescence of rare earth doped LaF_3 nanocrystals*

Wang Yan(王 艳)[b], Qin Wei-Ping(秦伟平)[a)b)†], Di Wei-Hua(狄卫华)[b], Zhang Ji-Sen(张继森)[b], and Cao Chun-Yan(曹春燕)[b]

[a)] *State Key Laboratory on Integrated Optoelectronics, College of Electronic Science and Engineering, Jilin University, Changchun* 130012, *China*

[b)] *Key Laboratory of Excited State Processes, Changchun Institute of Optics, Fine Mechanics and Physics, Chinese Academy of Sciences, Changchun* 130033, *China*

(Received 17 January 2008; revised manuscript received 25 February 2008)

This paper reports that hexagonal-phase LaF_3:$Yb^{3+}_{0.20}$, $Er^{3+}_{0.02}$ and LaF_3:$Yb^{3+}_{0.20}$, $Tm^{3+}_{0.02}$ nanocrystals (NCs) were synthesized via a hydrothermal method. The transmission electron microscopy, selected area electron diffraction, powder x-ray diffraction, and thermogravimetric analysis are used to characterize the NCs. Under 980 nm excitation, the Yb^{3+}/Er^{3+} and Yb^{3+}/Tm^{3+} codoped NCs colloidal solutions present bright green and blue upconversion fluorescence, respectively. These NCs show efficient infrared-to-violet and infrared-to-visible upconversion. The upconversion fluorescence mechanisms of LaF_3:$Yb^{3+}_{0.20}$, $Er^{3+}_{0.02}$ and LaF_3:$Yb^{3+}_{0.20}$, $Tm^{3+}_{0.02}$ NCs are investigated with a 980-nm diode laser as excitation source.

Keywords: upconversion fluorescence, infrared-to-visible, infrared-to-violet, nanocrystals
PACC: 3250F, 7855

1. Introduction

Lanthanide-doped upconversion fluorescence nanocrystals (NCs) have attracted considerable attention due to their potential applications in optics,[1,2] communication,[3] catalysis fields,[4] and in biological labelling.[5−7] Upconversion is a process which can absorb low-energy infrared light to produce high-energy visible or violet emission. Excited state absorption (ESA) and energy transfer (ET) can be a very efficient upconversion mechanism in rare-earth (RE) doped materials.[8,9] Codoping of Yb^{3+} as a sensitizer has yielded a substantial improvement in the upconversion efficiency in RE^{3+} (RE = Tm, or Er) doped systems due to the efficient ET between the sensitizer and RE ions.[10−12]

It is well known that the luminescence of RE ions is highly sensitive to the components and the structures of host materials. The upconversion fluorescence from RE ions is very easily quenched by high energy vibrations originated from host matrix. LaF_3,[3,13−16] usually possessing low phonon energy, is frequently considered as promising host matrix to minimize the quenching effect and increase upconversion fluorescent efficiency.[16,17] Recently, van Veggel *et al* prepared LaF_3 NCs using citrate or phosphate monoester based ligands.[18,19] Wang *et al* synthesized water soluble LaF_3 nanocrystals without using any ligands.[20] Yi and Chow obtained multicolour upconversion LaF_3 NCs by adding citrate ligands.[13] However, the upconversion luminescence, as demonstrated in a limited number of $NaYF_4$ samples,[5,21−27] in LaF_3 NCs colloidal solutions have not been reported, to the best of our knowledge. Li synthesized the oil soluble LaF_3 NCs with oleic acid as capping ligands.[15] However, they have not investigated the upconversion luminescent properties in LaF_3 host. On the other hand, in Yb^{3+}-sensitized RE doped upconversion NCs, efficient infrared to ultraviolet (UV) or violet upconversion emissions at room temperature have been rarely observed or investigated.

Herein, in this paper, we present a study on the colloidal LaF_3:$Yb^{3+}_{0.20}$, $Er^{3+}_{0.02}$ NCs with green upconversion fluorescence as well as on the colloidal LaF_3:$Yb^{3+}_{0.20}$, $Tm^{3+}_{0.02}$ NCs with blue upconversion fluorescence. The efficient infrared to ultraviolet, violet or visible upconversion emissions have been investigated.

*Project supported by the National Natural Science Foundation of China (Grant Nos 10474096 and 50672030).
†Corresponding author. E-mail: wpqin@jlu.edu.cn

2. Experimental

In a typical preparation, 0.12 mol oleic acid, 0.06 mol NaOH, 20 mL ethanol and 4 mL deionized water were mixed together under stirring. Then 2 mL 1.5 mol/L KF and 2-mL 0.5 mol/L $Ln(NO_3)_3$ (Ln=0.78 mmol La^{3+}, 0.20 mmol Yb^{3+}, and 0.02 mmol Er^{3+} or Tm^{3+}) were added into above solution. The mixture was agitated for another 30 min and then transferred to two 50 mL autoclave, sealed, and treated at 160°C for 16 h. Subsequently, the mixture was allowed to cool to room temperature, and the NCs were centrifugated, washed and dried.

The size and morphology of LaF_3:$Yb^{3+}_{0.20}$, $Er^{3+}_{0.02}$ were characterized by transmission electron microscopy (TEM) (JEM, 2000EX 200KV). The sample was prepared by placing a drop of dilute cyclohexane dispersion of NCs on a carbon film supported on a copper grid. Phase identification was performed via x-ray diffractometry (model Rigaku RU-200b), using nickel-filtered CuKα radiation (λ=0.15406 nm). The thermal behaviour of the nanocrystals was investigated using a thermogravimetric analyser (Perkin-Elmer TGA7). The curves were obtained with the sample in nitrogen atmosphere at the heating rate of 10°C/min. The upconversion emission spectra were performed with a Hitachi F-4500 fluorescence spectrometer. A power-adjustable laser diode (980 nm, 0 to 2 W, Beijing Hi-Tech Optoelectronic Co. China) with a lens making the beam parallel was employed as the excitation source. Under the excitation, upconversion fluorescent photos of the colloidal solutions were taken with a digital camera.

3. Results and discussion

The characterization data of as-synthesized powders are shown in Fig.1. Figure 1(a) displays TEM image of LaF_3:$Yb^{3+}_{0.20}$, $Er^{3+}_{0.02}$ nanoparticles with excellent dispersivity. Most particles present hexagonal profiles or show apparently crystal facets, indicating that they are single crystals. The electronic diffraction pattern (inset in Fig.1(a)), obvious rings made of bright dots, further confirms that the resulting nanoparticles are well crystallized. X-ray diffraction (XRD) investigations reveal that as-obtained materials are pure hexagonal LaF_3 crystals (JCPDS standard card, 84-0691), as shown in Fig.1(c). From the particle size distribution (Fig.1(b)), one can see that their diameters vary from 4 to 14 nm with 7.3 nm average size. The broadening of XRD peaks also indicates the small particle sizes. In our previous report, we have synthesized LaF_3 NCs at 180°C for 16 h.[28] From that TEM, we can see that the particle size is large. After lowering the synthetical temperature to 160°, we obtain the nearly monodisperse NCs with small size (smaller than 10 nm). As we know, small particle size (usually smaller than 10 nm) and excellent dispersivity are essential to form transparent colloidal solution and to exploit the potential biological labelling applications of luminescent nanoparticles. The higher is the reaction temperature, the faster is the growth rate of nuclei, which results in the larger size of NCs. Therefore, the preferential reaction temperature is 160°C to prepare nearly monodisperse LaF_3 NCs using hydrothermal method with oleic acid as ligand.

(a)

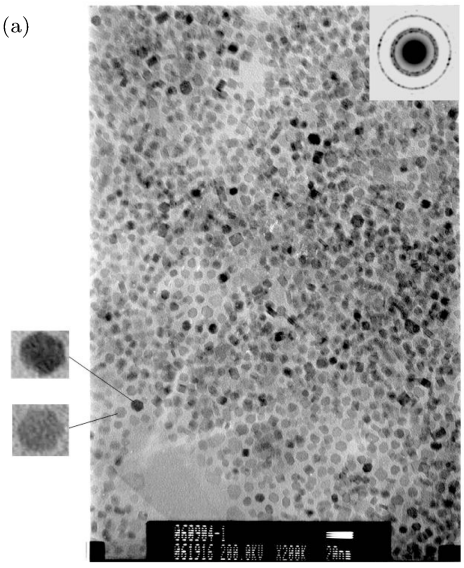

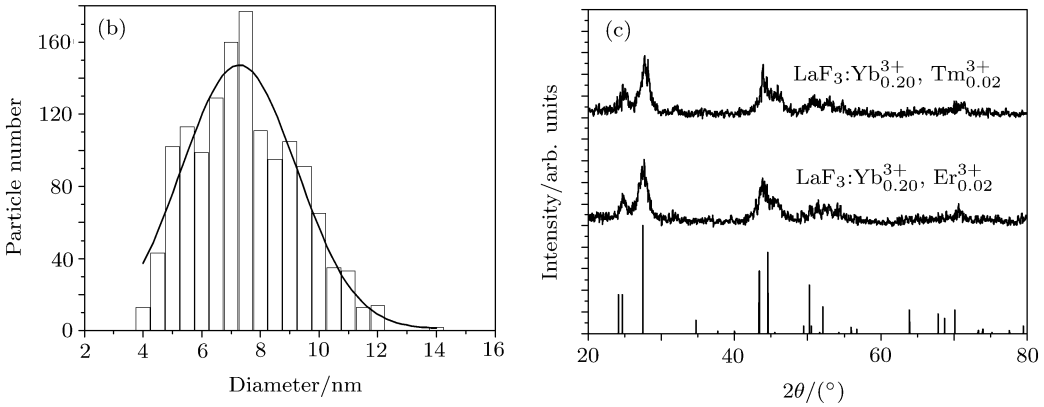

Fig.1. Characterization data for LaF_3 NCs. (a) TEM image of $LaF_3:Yb^{3+}_{0.20}$, $Er^{3+}_{0.02}$ with a 20-nm scale bar. Inset: The electronic diffraction of $LaF_3:Yb^{3+}_{0.20}$, $Er^{3+}_{0.02}$ NCs. Left: Two amplified NCs with crystal facets. (b) Statistical histogram of the particle sizes obtained from 1400 NCs in TEM image. (c) Powder XRD patterns.

Figure 2 shows photographs of $LaF_3:Yb^{3+}_{0.20}$, $Er^{3+}_{0.02}$ and $LaF_3:Yb^{3+}_{0.20}$, $Tm^{3+}_{0.02}$ NC solutions in cyclohexane with the same concentration of 50 mg/mL. The colloidal solutions are transparent (Figs.2(A) and 2(B)). Owing to the presence of the oleic acid, the NCs can be re-dispersed in nonpolar solvents and colloidally steadied for a long time without any visible precipitate. The presence of the oleic acid ligands was confirmed by thermogravimetric analysis (TGA), as shown in Fig.3. Figure 2(C) and 2(D) show eye-visible upconversion luminescence under 980-nm excitation with a pump power density about 100 W/cm^2. It is worth noting that this is the first report which gives the upconversion fluorescence photo from RE doped LaF_3 NC colloidal solution.

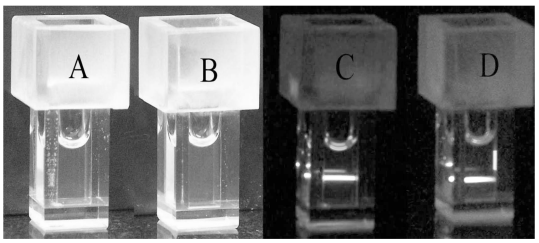

Fig.2. Upconversion luminescence of nanocrystal colloidal solutions in cyclohexane excited at 980 nm with a pump power density about 100 W/cm^2, and the concentration is 50 mg/mL. (A) and (B) Transparent $LaF_3:Yb^{3+}_{0.20}$, $Er^{3+}_{0.02,}$ and $LaF_3:Yb^{3+}_{0.20}$, $Tm^{3+}_{0.02}$ solutions. (C) Upconversion luminescence of $LaF_3:Yb^{3+}_{0.20}$, $Er^{3+}_{0.02}$ solution and (D) Upconversion luminescence of $LaF_3:Yb^{3+}_{0.20}$, $Tm^{3+}_{0.02}$ under 980-nm excitation. The capacity of one cell is 1 mL.

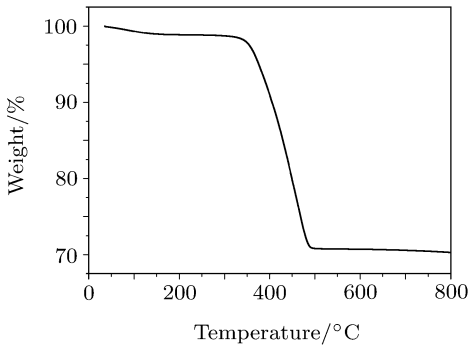

Fig.3. TGA of $LaF_3:Yb^{3+}_{0.20}$, $Er^{3+}_{0.02}$ NCs powder.

The room-temperature upconversion spectra of $LaF_3:Yb^{3+}_{0.20}$, $Er^{3+}_{0.02}$ and $LaF_3:Yb^{3+}_{0.20}$, $Tm^{3+}_{0.02}$ NCs are presented in Fig.4. For $LaF_3:Yb^{3+}_{0.20}$, $Er^{3+}_{0.02}$ NCs, under 980-nm excitation, four emission peaks have been recorded in the visible region. They are assigned to $^2H_{9/2} \rightarrow {}^4I_{15/2}$ (408.6 nm), $^2H_{11/2} \rightarrow {}^4I_{15/2}$ (520.4 nm), $^4S_{3/2} \rightarrow {}^4I_{15/2}$ (541.8 nm) and $^4F_{9/2} \rightarrow {}^4I_{15/2}$ (651.2 nm) transitions of Er^{3+} ions, respectively.[8,29−31] Obviously, the green emission is dominant (92%) in the upconversion fluorescence; the blue and the red upconversion emissions are very weak. This suggests that the $LaF_3:Yb^{3+}_{0.20}$, $Er^{3+}_{0.02}$ NCs may be a promising candidate for green labelling applications. For the $LaF_3:Yb^{3+}_{0.20}$, $Tm^{3+}_{0.02}$ NCs, the blue emission bands at 473.2 nm and 450.8 nm correspond to the transitions from $^1G_4 \rightarrow {}^3H_6$ and $^1D_2 \rightarrow {}^3F_4$, respectively.[5,26] Therefore, the upconversion fluorescence from the Yb/Tm solution exhibits pure blue.

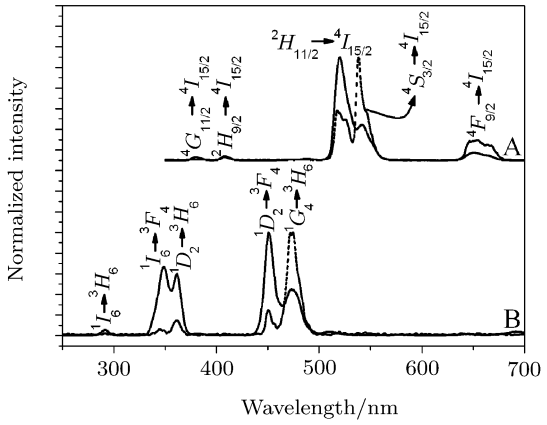

Fig.4. Upconversion emission spectra of NCs excited at 980 nm and 100 W/cm^2. (A) LaF_3:$Yb^{3+}_{0.20}$, $Er^{3+}_{0.02}$ and (B) LaF_3:$Yb^{3+}_{0.20}$, $Tm^{3+}_{0.02}$. (Black short dash: Upconversion emission spectra recorded with the pump power density of 20 W/cm^2).

Except visible emissions, violet and UV emissions also present in the emission spectra, corresponding to the transitions of $^4G_{11/2} \rightarrow {}^4I_{15/2}$ (380 nm) for LaF_3:$Yb^{3+}_{0.20}$, $Er^{3+}_{0.02}$ and $^1I_6 \rightarrow {}^3H_6$ (290 nm), $^1I_6 \rightarrow {}^3F_4$ (348 nm), $^1D_2 \rightarrow {}^3H_6$ (361.6 nm) for LaF_3:$Yb^{3+}_{0.20}$, $Tm^{3+}_{0.02}$.[8,9,32] For an unsaturated upconversion process, the fluorescent intensity, I_s, is proportional to I^n_{pump}, where I_{pump} is the 980-nm excitation intensity and the integer n is the number of photons absorbed in one upconversion emission process. In Fig.5, we give the intensity dependences of upconverted fluorescence on the pump power at 980 nm. Each integer n is determined from the slope of corresponding line in bi-logarithmic coordinates, as shown in Figs.5(a) and 5(b). The slopes are fitted as 1.89, 1.74, 1.82, and 2.95 for the LaF_3:$Yb^{3+}_{0.20}$, $Er^{3+}_{0.02}$ NCs and 2.70, 3.98, 3.96, 4.73, and 4.59 for the LaF_3:$Yb^{3+}_{0.20}$, $Tm^{3+}_{0.02}$ NCs, respectively. Hereby, the upconversion emissions are two-photon or three-photon processes for Yb/Er solution and three-photon, four-photon or five-photon processes for Yb/Tm solution, as shown in Fig.6. In Yb/Er co-doped system, the upconversion emission may be resulted from different processes, including ESA, ET between neighbouring excited Er^{3+} ions, and APTE (addition de photons par transfer d'Energie) between Yb^{3+} and Er^{3+} ions. Among them, APTE is the most efficient. Under 980 nm excitation, the violet, green and red upconversion emission in LaF_3:$Yb^{3+}_{0.20}$, $Er^{3+}_{0.02}$ NCs would produce as follows.[8,33]

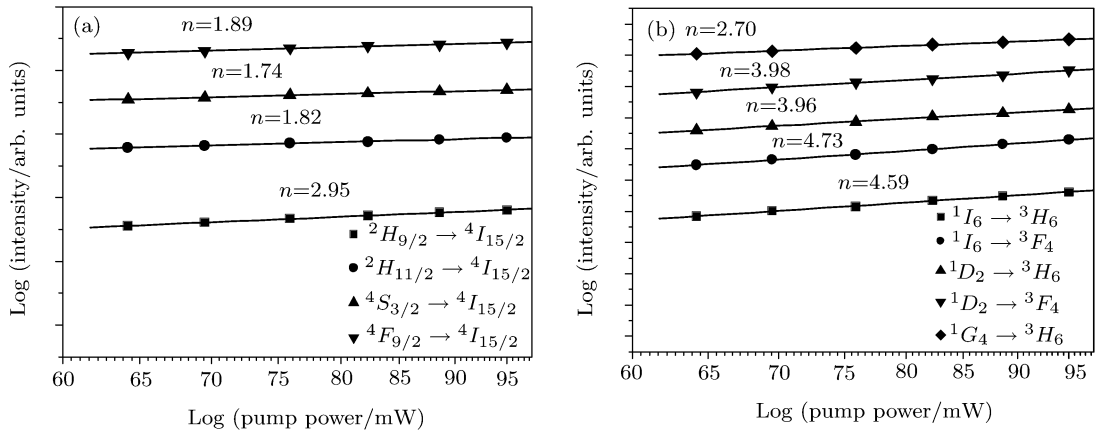

Fig.5. Intensity dependences of the up-converted fluorescence on the pump power excited at 980 nm. (a) LaF_3:$Yb^{3+}_{0.20}$, $Er^{3+}_{0.02}$, and (b) LaF_3:$Yb^{3+}_{0.20}$, $Tm^{3+}_{0.02}$.

Green emission: $^2F_{5/2} \rightarrow 2F_{7/2}$ (Yb^{3+}): $^4I_{15/2} \rightarrow {}^4I_{11/2}$ ($Er3^+$), $^2F_{5/2} \rightarrow {}^2F_{7/2}$ (Yb^{3+}): $^4I_{11/2} \rightarrow {}^4F_{7/2}$ (Er^{3+}), $^4F_{7/2} \rightarrow {}^2H_{11/2}$, $^4S_{3/2}$ (Er^{3+}) (non-radiative relaxation).

Red emission: $^2F_{5/2} \rightarrow {}^2F_{7/2}$($Yb^{3+}$): $^4I_{15/2} \rightarrow {}^4I_{11/2}$ (Er^{3+}), $^4I_{11/2} \rightarrow {}^4I_{13/2}$ (non-radiative relaxation), $^2F_{5/2} \rightarrow {}^2F_{7/2}$ (Yb^{3+}): $^4I_{13/2} \rightarrow {}^4F_{9/2}$ (Er^{3+}).

Violet emission: (process 1) $^2F_{5/2} \rightarrow {}^2F_{7/2}$ (Yb^{3+}):$^4F_{9/2} \rightarrow {}^2H_{9/2}$ (Er^{3+}); (process 2) $^2F_{5/2} \rightarrow {}^2F_{7/2}$ (Yb^{3+}):$^4S_{3/2} \rightarrow {}^2G_{7/2}$ (Er^{3+}), $^2G_{7/2} \rightarrow {}^4G_{11/2}$, $^2H_{9/2}$ (non-radiative relaxation). On the other hand, the following cross relaxation, $^4G_{11/2} \rightarrow {}^4F_{9/2}$ (Er^{3+}):$^2F_{7/2} \rightarrow {}^2F_{5/2}$($Yb^{3+}$), would depopulate the state $^4G_{11/2}$.[34]

In Yb^{3+}/Tm^{3+} co-doped systems, different process may result in upconversion. According to the energy level diagrams of Tm^{3+} and Yb^{3+}, the pump light excites only the Yb^{3+} ions and three successive energy transfers from Yb^{3+} to Tm^{3+} populate $^3H_5$, ($^3F_3$, $^3F_2$), and $^1G_4$. Owing to the large energy

mismatch ($3516\,\mathrm{cm}^{-1}$) in the transfer $^2F_{5/2} \rightarrow {}^2F_{7/2}$ (Yb^{3+}):$^1G_4 \rightarrow {}^1D_2$ (Tm^{3+}), the process $^3F_2 \rightarrow {}^3H_6$ (Tm^{3+}): $^3H_4 \rightarrow {}^1D_2$ (Tm^{3+}) may alternatively play the most important role in populating $^1D_2$. Thereafter, the state $^1I_6$ can be populated by $^2F_{5/2} \rightarrow {}^2F_{7/2}$ (Yb^{3+}):$^1D_2 \rightarrow {}^1I_6$ (Tm^{3+}).[9,35,36] In addition, we also found that high-order (5-photon and 4-photon) upconversion processes occurs sensitively on pump power densities and can be easily avoided or enhanced by choosing a proper pump level, as shown in Fig.4. In our previous reports, we concluded that the high efficiency of five-photon, four-photon upconversion emissions came from the change of Judd–Ofelt parameters $\Omega_{2,4}$ in pulsed-laser deposition (PLD) particles.[8,9,37] There, the pulsed laser distorted the crystal structures in PLD particles. However, the five-photon and four-photon (NIR-to-UV or NIR-to-violet) upconversion processes are also very efficient in our LaF_3: RE colloidal solutions. Presumably, we ascribe this phenomenon to the high crystallization of LaF_3: RE NCs, low phonon energy. The high-order upconversion emissions from LaF_3 NCs exhibit its excellent upconversion ability.

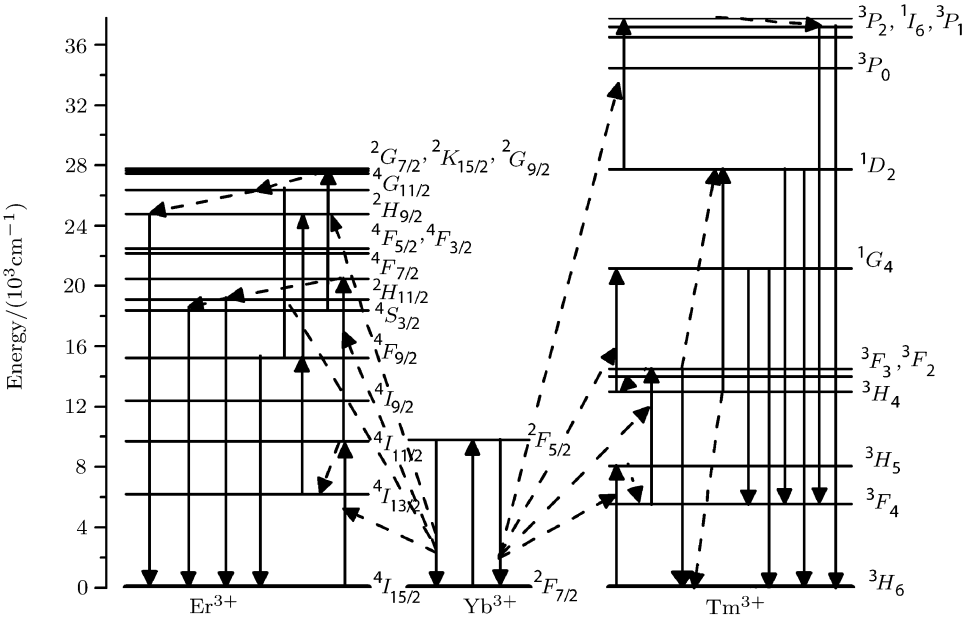

Fig.6. Excitation and emission schemes for Yb^{3+}/Er^{3+} and Yb^{3+}/Tm^{3+} systems.

4. Conclusions

In conclusion, we have synthesized hexagonal-phase LaF_3 NCs codoped with Yb^{3+}/Er^{3+} or Yb^{3+}/Tm^{3+} using a simple method. The LaF_3: RE^{3+} NCs colloidal solutions exhibit bright upconversion fluorescence under 980-nm excitation. The NCs show efficient IR-to-violet or IR-to-visible upconversion. These NCs have potential applications in biosensors, display and short-wavelength lasers based on the upconversion principle.

References

[1] Riwotzki K, Meyssamy H, Schnablegger H, Kornowski A and Haase M 2001 *Angew. Chem. Int. Ed.* **40** 573

[2] Heer S, Lehmann O, Haase M and Güdel H U 2003 *Angew. Chem. Int. Ed.* **42** 3179

[3] Stouwdam J W and van Veggel F C J M 2002 *Nano Lett.* **2** 733

[4] Zhou K, Wang X, Sun X M, Peng Q and Li Y 2005 *J. Catal.* **229** 206

[5] Heer S, Kömpe K, Güdel H U and Haase M 2004 *Adv. Mater.* **16** 2102

[6] Aebischer A, Heer S, Biner D, Krämer K, Haase M and Güdel H U 2005 *Chem. Phys. Lett.* **407** 124

[7] Wang L, Yan R, Huo Z, Wang L, Zeng J, Bao J, Wang X, Peng Q and Li Y 2005 *Angew. Chem. Int. Ed.* **44** 6054

[8] Qin G, Qin W, Huang S, Wu C, Zhao D, Chen B, Lü S and Shulin E 2002 *J. Appl. Phys.* **92** 6936
[9] Qin G, Qin W, Wu C, Huang S, Zhang J, Lü S, Zhao D and Liu H 2003 *J. Appl. Phys.* **93** 4328
[10] Zou X and Toratani H 1995 *J. Non-Cryst. Solids* **181** 87
[11] Tsuboi T 2000 *Phys. Rev.* B **62** 4200
[12] Oliveira A S, Gouveia E A, de Araujo M T, Gouveia-Neto A S, de Araujo Cid B and Messaddeq Y 2000 *J. Appl. Phys.* **87** 4274
[13] Yi G S and Chow G M 2005 *J. Mater. Chem.* **15** 4460
[14] De G J H, Qin W, Zhang J, Zhao D and Zhang J 2005 *Chem. Lett.* **34** 914
[15] Wang X, Zhuang J, Peng Q and Li Y 2006 *Inorganic Chemistry* **45** 6661
[16] Diamente P R, Burke R D and van Veggel F C J M 2006 *Langmuir* **22** 1782
[17] Yan R and Li Y 2005 *Adv. Func. Mater.* **15** 763
[18] Sudarsan V, van Veggel F C J M, Herring R A and Raudsepp M 2005 *J. Mater. Chem.* **15** 1332
[19] Diamente P R and van Veggel F C J M 2005 *J. Fluoresc.* **15** 543
[20] Wang F, Zhang Y, Fan X and Wang M 2006 *J. Mater. Chem.* **16** 1031
[21] Boyer J C, Vetrone F, Cuccia L A and Capobianco J A 2006 *J. Am. Chem. Soc.* **128** 7444
[22] Yi G S and Chow G M 2006 *Adv. Func. Mater.* **16** 2324
[23] Wang L Y and Li Y 2006 *Nano Lett.* **6** 1645
[24] Li Z Q and Zhang Y 2006 *Angew. Chem. Int. Ed.* **45** 7732
[25] Yi G S and Chow G M 2007 *Chem. Mater.* **19** 341
[26] Wang L and Li Y 2007 *Chem. Mater.* **19** 727
[27] Schäfer H, Ptacek P, Kömpe K and Haase M 2007 *Chem. Mater.* **19** 1396
[28] Wang Y, Qin W, Zhang J, Cao C, Zhang J, Jin Y, Zhu P, Wei G, Wang G and Wang L 2007 *Chem. Lett.* **36** 912
[29] Dai S ,Li X, Nie Q, Shen X, Wang X and Xu T 2007 *Acta Phys. Sin.* **56** 5518 (in Chinese)
[30] Dai Z, Yang H and Zu N 2007 *Chin. Phys.* **16** 1650
[31] Jiang Z, Li T and Zhang Q 2007 *Chin. Phys.* **16** 1155
[32] Dai S, Duan Z, He D, He L and Zhang J 2006 *Chin. Phys.* **15** 209
[33] Qin G, Qin W, Wu C, Zhao D, Zhang J, Lü S, Huang S and Xu W 2004 *J. Non-Crystalline Solids* **347** 52
[34] Wang Y and Ohwaki J 1993 *Appl. Phys. Lett.* **63** 3268
[35] Thrash R J and Johnson L F 1994 *J. Opt. Soc. Am.* B **11** 881
[36] Qin G, Qin W, Wu C, Huang S, Zhao D, Zhang J and Lü S 2004 *Opt. Commun.* **242** 215
[37] Qin W, Qin G, Chung Y, Lee Y, Kim C and Jang K 2004 *J. Korean Phys. Soc.* **44** 925